# Metallophilic Interactions in Closed-Shell $d^{10}$ Metal−Metal Dicyanide Bonded Luminescent Systems $Eu[Ag_xAu_{1-x}(CN)_2]_3$ and Their Tunability for Excited State Energy Transfer

**Julie Clarissa F. Colis,[†] Richard Staples,[‡] Carl Tripp,[†,§] David Labrecque,[†] and Howard Patterson*[,†]**

*Department of Chemistry, University of Maine, Orono, Maine 04469, Department of Chemistry and Chemical Biology, Harvard University, Cambridge, Massachusetts 02138, and Laboratory for Surface Science and Technology, University of Maine, Orono, Maine 04469*

*Received: July 23, 2004; In Final Form: October 14, 2004*

We report on the heterobimetallic system, $Eu[Ag_xAu_{1-x}(CN)_2]_3$ ($x = 0-1$) in which sensitization of europium luminescence occurs by energy transfer from $[Ag_xAu_{1-x}(CN)_2]^-$ donor excited states. The donor states have energies which are tunable and dependent on the Ag/Au stoichiometric ratio. These layered systems exhibit interesting properties, one of which is their emission energy tunability when excited at different excitation wavelengths. In this paper, we report on their use as donor systems with Eu(III) ions as acceptor ions in energy transfer studies. Luminescence results show that the mixed metal dicyanides with the higher silver loading have a better energy transfer efficiency than the pure $Ag(CN)_2^-$ and $Au(CN)_2^-$ donors. The better energy transfer efficiency is due to the greater overlap between the donor emission and acceptor excitation. Additionally, more acceptor states are available in the high silver loading mixed metal Eu(III) complexes. The results from a crystal structure determination and Raman experiments are also presented in this paper and provide information about metallophilic interactions in the closed-shell $d^{10}$ metal−metal $[Ag_xAu_{1-x}(CN_2]^-$ dicyanide clusters.

## 1. Introduction

The discovery of interesting optical properties of the mixed metal dicyanides has prompted energy transfer studies using the mixed metal species as the donor system. Our group has reported a comparison between Au−Au and Ag−Ag interactions in the ground and excited states of dicyano complexes.[1] These studies of cyano complexes of Au(I) and Ag(I) relate the photoluminescence properties of the systems to the formation of metal−metal bonded excimers and exciplexes. The optical phenomenon of "exciplex" tuning has been found to be a characteristic property of dicyanoargentate and dicyanoaurate compounds. Emission energies of these systems can be tuned by varying certain physical parameters, such as temperature,[2] pressure,[3] excitation wavelength,[4] and dopant concentration.[4b,5] The rich optical properties of the $d^{10}$ gold and silver metals have prompted our group to extend investigations to mixed-metal systems. As reported[6] in another paper on complexes with La(III) ion as the cation, the mixed metal dicyanides have been found to have emission energy tunability when the Ag/Au stoichiometric ratio is varied. Strong luminescence intensity at ambient temperatures of the mixed metal dicyanides have also been observed. Tunability of the excited state properties is extremely important in a variety of optoelectronic applications in relation to some fundamental scientific issues such as excitonic energy transfer.[7−9] The tunability of mixed metal dicyanides makes them good candidates for donors in energy transfer studies.

Studies on the optical properties of rare earth elements are strongly motivated by their unique luminescence characteristics, such as long luminescence lifetimes and line-like emission of the lanthanide ions.[10] Complexes containing the rare earth ions emit over the entire spectral range of interest: near-infrared (NIR: $Nd^{3+}$, $Er^{3+}$), red ($Eu^{3+}$, $Pr^{3+}$, $Sm^{3+}$), green ($Er^{3+}$, $Tb^{3+}$), and blue ($Tm^{3+}$, $Ce^{3+}$).[25] These properties make lanthanide ions attractive for applications in solid-state photonic devices.[11]

Optical transitions in these rare earth complexes involve the 4f orbitals which are well shielded from their chemical environment by $5s^2$ and $5p^6$ electrons. Since f−f transitions are parity forbidden, the absorption coefficients are very low and the emissive states are long-lived, resulting in long-lived and line-like emission bands. Due to low extinction coefficients of the lanthanide ions, their direct excitation is unfavorable. Furthermore, comparatively fast relaxation of the excitation energy is a problem when using lanthanide ions for luminescence.[12] To overcome the difficulties of low absorptivity, sensitizers which allow excitation in the near UV/vis region have been incorporated in lanthanide complexes. The sensitizer/donor (S) component absorbs the exciting radiation and subsequently transfers it to the lanthanide ion (A, acceptor). Examples of sensitizers used in energy transfer studies in rare earth systems are antennae,[13] matrices,[14] films,[15] nanocrystals,[16] organic molecules,[17] phosphors such as $Y_2O_3$,[18] and nanoclusters.[19] For faster energy transfer, a short distance between the donor ion and the lanthanide ion is desirable. The degree of energy transfer is highly dependent on the spectral overlap between the donor emission and the acceptor absorption; therefore, the donor's tunability can result in very strong sensitized luminescence from a variety of the europium energy levels.

The objective of this paper is to report on studies that investigate energy transfer processes and metallophilic interac-

* To whom correspondence should be addressed. E-mail: howardp@maine.edu.
[†] Department of Chemistry, University of Maine.
[‡] Harvard University.
[§] Laboratory for Surface Science and Technology, University of Maine.

10.1021/jp046717g CCC: $30.25 
Published on Web 12/09/2004

**TABLE 1: Computed Au/Ag Ratio in the Mixed Metal Europium Ion Single Crystals**

| mother solution | computed loading based on Raman measurements | empirical formula from X-ray studies |
|---|---|---|
| $Eu[Ag(CN)_2]_3$ | | $Eu[Ag(CN)_2]_3 \cdot 3H_2O$[a] |
| $Eu[Ag_{0.90}Au_{0.10}(CN)_2]_3$ | $Eu[Ag_{0.85}Au_{0.15}(CN)_2]_3$ | |
| $Eu[Ag_{0.75}Au_{0.25}(CN)_2]_3$ | $Eu[Ag_{0.66}Au_{0.34}(CN)_2]_3$ | |
| $Eu[Ag_{0.50}Au_{0.50}(CN)_2]_3$ | $Eu[Ag_{0.35}Au_{0.65}(CN)_2]_3$ | |
| $Eu[Ag_{0.25}Au_{0.75}(CN)_2]_3$ | $Eu[Ag_{0.18}Au_{0.82}(CN)_2]_3$ | $Eu[Ag_{0.14}Au_{0.86}(CN)_2]_3 \cdot 3H_2O$ |
| $Eu[Au(CN)_2]_3$ | | |

[a] Data taken from ref 33.

tions in $Eu[Ag_xAu_{1-x}(CN)_2]_3$ $x$=0.90, 0.75, 0.50, and 0.25. This is a heterobimetallic layered system which is novel because the $\{Ag_xAu_{1-x}\}^-$ donor ions exhibit tunability for excited-state energy transfer dependent on the Ag/Au stoichiometric ratio.

## 2. Results and Discussion

**2.1. Synthesis.** Six europium ion complexes were prepared: $Eu[Ag_xAu_{1-x}(CN)_2]_3$, $x$ = 1, 0.90, 0.75, 0.50, 0.25, and 0. Hexagonally shaped crystals were harvested 14−21 days after preparation. Pure $Eu[Au(CN)_2]_3$ and $Eu[Ag_{0.25}Au_{0.75}(CN)_2]_3$ crystals are canary yellow in color and the rest of the crystals in the series with smaller amounts of gold are colorless. Several other rare earth-silver dicyanide systems under investigation in the laboratory are also colorless. The technique used[6] in the determination of the Ag/Au loading in the lanthanum crystals was used for the Eu complexes since it provided a quick and nondestructive method. Moreover, the method allows for the determination of the Ag/Au loadings for crystal samples which are not suitable for X-ray studies. In this technique, the Au/Ag ratio of the samples was computed by integration of the CN stretch peak areas taken from Raman measurements. Table 1 shows the computed values from Raman data of Ag/Au loading in the Eu complexes. Comparing the computed Au/Ag ratio for the single crystals of the mixed metal europium complex with that of the precursor, it is observed that there is higher loading of the gold ions versus that of the silver ions in the crystals formed compared to the Ag/Au ratio in the starting materials. This has also been observed in the La complexes.

**2.2. Structural Studies.** Dicyanoaurate and dicyanoargentate compounds have been the subject of increasing interest due to their two-dimensional layered structures and their interesting emission properties.[21−29] These structures consist of layers of $[M(CN)_2]^-$ M = Au and Ag complexes alternating with layers of $Ln^{+3}$ ions Ln = $La^{3+}$, $Eu^{3+}$, and $Tb^{3+}$, which are in several cases coordinated with water molecules.[20a,30−32] The characterization of the Eu mixed metal complexes has been carried out to elucidate the correlation between the spectroscopic and structural properties. The crystal structure of the pure $Eu[Ag(CN)_2]_3$ has been solved.[33] It belongs to the hexagonal system and has the $P6_3/mcm$ (#193) space group. The Eu−N distance is 2.539(4) Å which indicate the strong bonding interaction between the Eu atom and the $CN^-$ ligands. The C−N distance is 1.144(6) Å and the Ag−C distance is 2.059(5) Å. The bond distances are significant since they influence the degree of energy transfer between the donor and the acceptor units. This is exemplified in energy transfer studies that use antenna units[13] and matrices[14] as sensitizers. The crystal structure of pure $Eu[Au(CN)_2]_3$ has not been determined but preliminary studies report[3] it to have the space group P62m (#189).

Among the four mixed metal Eu complexes that have been prepared, only the crystal structure of $Eu[Ag_{0.14}Au_{0.86}(CN)_2]_3$ (precursor Ag/Au loading) has been solved. Crystallographic data is found in Table 2. The complex crystallizes with three

**TABLE 2: Summary of Crystallographic Data[a]**

| | $Eu[Ag_{0.14}Au_{0.86}(CN)_2]_3 \cdot 3H_2O$ |
|---|---|
| empirical formula | $C_6H_6Ag_{0.41}Au_{2.59}EuN_6O_3$ |
| Fw | 916.50 |
| $a$, Å | 6.5750(8) |
| $b$, Å | 6.5750(8) |
| $c$, Å | 18.440(3) |
| α, deg | 90 |
| $\beta$, deg | 90 |
| $\gamma$, deg | 120 |
| V, Å$^3$ | 690.38(17) |
| Z | 2 |
| crystal system | hexagonal |
| space group | $P6_3/mcm$ |
| $T$, K | 293(2) |
| $\lambda$, Å | 0.71073 |
| $\rho$, Mg/m$^3$ | 4.409 |
| $\mu$, mm$^{-1}$ | 32.496 |
| $R1$[b] | 0.0327 |
| wR2[c] | 0.0771 |

[a] Obtained with graphite monochromated Mo Kα ($\lambda$ = 0.71073 Å) radiation. [b] $R1 = \sum||F_o| - |F_c||/\sum|F_o|$ [c] $wR_2$ $\{\sum[w(F_o^2 - F_c^2)^2]/\{\sum[w(F_o^2)^2]\}^{1/2}$.

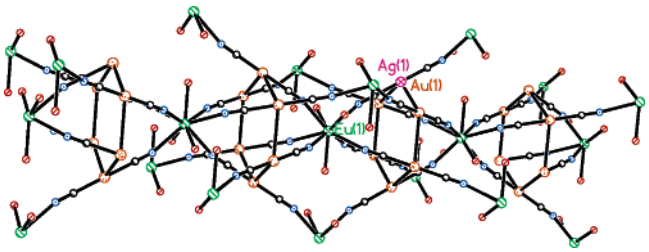


**Figure 1.** $Eu[Ag_{0.14}Au_{0.86}(CN)_2]_3$*$3H_2O$. Drawing (50% probability ellipsoids) of $Eu[Ag_{0.14}Au_{0.86}(CN)_2]_3$*$3H_2O$. The Au- - -Au distance is 3.2875(4) Å Selected distances: Au−C(1), 2.009(9) Å; N−C, 1.139-(13) Å; Eu−O, 2.433(11) Å; Eu−N, 2.559(8) Å. Selected bond angles: C−Au−C, 180.0(6)°; Au−C−N, 179.8(12)°; Eu−N−C, 165.4-(8)°. Large striped pink circles represent Ag atoms, large hatched green Eu atoms, small black C atoms, small blue N atoms, small striped orange O atoms and small blue-green H atoms.

water molecules in the space group $P6_3/mcm$ (#193). The Ag or Au atom resides on the inversion center (0, 1/2, 0) and this imposes a bond angle of 180°. The complex displays M−M interactions that forms a hexagonal array with diagonal interaction in the layer. This layer effect is along the $c$ axis which shows that the Ag or Au metal atoms alternate with the $Eu^{3+}$ ions. The metal atoms are arranged in layers perpendicular to the $c$ axis. Every metal atom has four nearest neighbors in a rectangular arrangement.

The europium ion is found residing on the $\bar{6}2m$ site (0, 0, 1/4) with the water molecule sitting on a mirror plane (x, −2x, 1/4). The europium ion is surrounded by three waters and six-coordinated CN, through the nitrogen. The environment of the $Eu^{3+}$ ions consists of six $CN^-$ groups coordinated approximately end-on, resulting in original prismatic geometry. Figure 1 shows the Eu ion layer with the water molecules also coordinated.

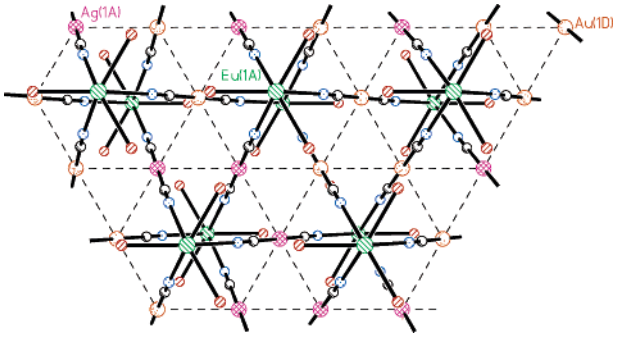


**Figure 2.** $Eu[Ag_{0.14}Au_{0.86}(CN)_2]_3 \cdot 3H_2O$. Drawing showing the Au- - -Ag interactions which form the hexagonal array and the trigonal geometry interactions in these complexes.

Three water molecules complete the recapped original prism. By symmetry, the three O atoms of the water molecules are coplanar with the $Eu^{3+}$ ion. The Eu−O distance is short; thus, the total coordination of $Eu^{3+}$ is nine. Although there exists a mirror plane along the plane that contains the three O atoms and the $Eu^{3+}$ ion, no perpendicular plane is evident. The Eu ion has essentially the $C_3$ symmetry. Figure 2 shows the complex with the display of the Au−Au interaction, with bond distance of 3.2875(4) Å.

**2.3. Raman Studies.** Raman scattering experiments have been carried out to complement structural studies on the characterization of the samples. The high and low-frequency regions of the Raman spectra for the samples are shown in Figure 3, parts a and b, respectively. Assignments of the Raman bands are given in Table 3. The Raman spectra of $Eu[Ag_xAu_{1-x}(CN)_2]_3$, $x = 0$, 0.25, 0.50, 0.75, 0.90, and 1, systems will be discussed by analogy with the Raman spectra of $KAu(CN)_2$ and $KAg(CN)_2$, which have been studied in detail.[34−37] In $KAu(CN)_2$ Raman studies,[36−38] bands are observed at ∼2160 $cm^{-1}$ (CN stretch) and at ∼305 $cm^{-1}$ (AuCN bend). In previous work,[36] the Au−C stretch has not been observed but has been assigned to be at 452 $cm^{-1}$, deduced from infrared combination bands. In the work of Adams and Fletcher,[37] the Au−C stretch has been reported although it was observed as an extremely weak and broad pair of bands at ca. 450 $cm^{-1}$. From a comparison to the literature, we assign bands for $Eu[Au(CN)_2]_3$ at 2176 $cm^{-1}$ to the CN stretching mode. In a study of a similar complex,[20b] $Dy[Au(CN)_2]_3$, it was reported that the CN stretching mode was observed at 2178 $cm^{-1}$. Raman bands at 332 and 350 $cm^{-1}$ are assigned to AuCN bending modes. A very weak Raman band has also been observed at 468 $cm^{-1}$ which is assigned to the AuC stretching frequency. In $KAg(CN)_2$ Raman studies,[34−37] fundamental bands are observed at ∼2140 $cm^{-1}$ (CN stretch) and at ∼250 $cm^{-1}$ (AgCN bend). Analogous to $KAu(CN)_2$, the Ag−C stretching frequency has been reported[35,36] to be absent or is extremely low in intensity. The Ag−C stretch has been assigned to be at ∼360 $cm^{-1}$, deduced from infrared-active combination bands.[35] Our measurements show that the $Eu[Ag(CN)_2]_3$ fundamental bands are at 2163 $cm^{-1}$ (CN stretch) and at 299 $cm^{-1}$ and 281 $cm^{-1}$ (AgCN bend). Two well-resolved peaks are observed at 415 and 385 $cm^{-1}$ which we assign as AgC stretching frequencies.

It was observed that there is a correlation between the relative intensities of the respective peaks from the $\nu$(CN) stretching mode arising from $Ag(CN)_2^-$ and $Au(CN)_2^-$ ions to the Ag

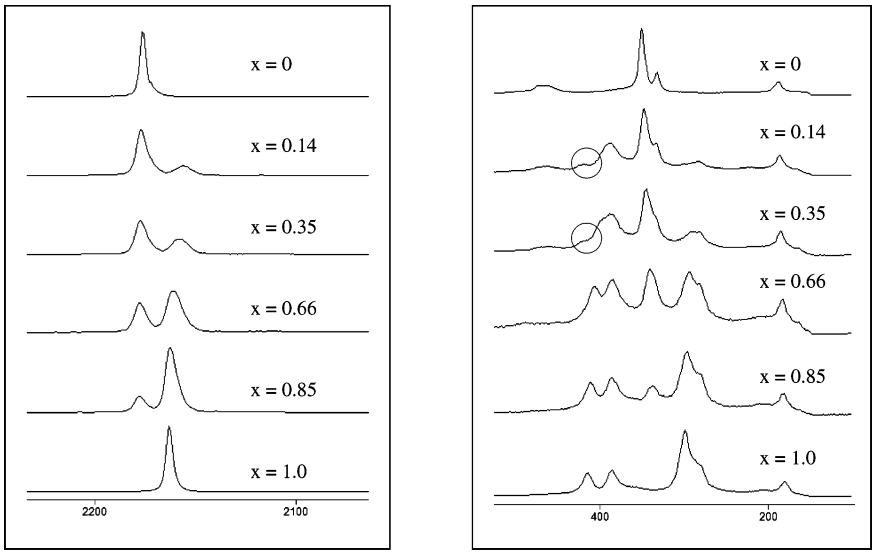


**Figure 3.** Raman shifts for $Eu[Ag_xAu_{1-x}(CN)_2]_3$, with $x = 1.0$, 0.85, 0.66, 0.35, 0.14, and 0; (a) C−N stretching frequency, (b) M-CN bending and M−C stretching region. Experimental conditions: laser excitation 785 nm at 298K.

**TABLE 3: Assignment of Raman Bands/Raman Shift, $cm^{-1}$**

| $Eu[Ag(CN)_2]_3$ | $Eu[Ag_{0.85}Au_{0.15}(CN)_2]_3$ | $Eu[Ag_{0.66}Au_{0.34}(CN)_2]_3$ | $Eu[Ag_{0.35}Au_{0.65}(CN)_2]_3$ | $Eu[Ag_{0.14}Au_{0.86}(CN)_2]_3$ | $Eu[Au(CN)_2]_3$ | assgnt |
|---|---|---|---|---|---|---|
| 2163 | 2162 | 2161 | 2158 | 2156 | | $\nu$(CN) |
| | 2178 | 2178 | 2177 | 2177 | 2176 | $\nu$(CN) |
| | | | | | 2172 | |
| | | | 468 | 468 | 468 | $\nu$(AuC) |
| 415 | 411 | 407 | 400 | | | $\nu$(AgC) |
| 385 | 385 | 384 | 387 | 388 | | |
| | 336 | 341 | 345 | 348 | 350 | $\delta$(AuCN) |
| | | | 334 | 333 | 332 | |
| 299 | 297 | 294 | 286 | 285 | | $\delta$(AgCN) |
| 281 | 281 | 282 | | | | |

and Au loading in the sample. In fact as mentioned earlier, the Ag/Au ratios in the mixed metal samples were computed by integration of the CN stretch peak areas. This method afforded a faster way to determine the Ag/Au ratio in the final product rather than have the crystal structure of each sample solved. Upon comparison to the empirical formulas resolved from X-ray studies of $Eu[Ag_{0.14}Au_{0.86}(CN)_2]_3$, it was found that the Ag/Au ratio solved from Raman data are in agreement with the empirical formulas. The Raman data therefore provides information on the Ag/Au loading in the other crystal systems whose structures were not solved by X-ray studies.

It is with the $\nu$(AgC) and $\nu$(AuC) modes that the influence of silver−gold interaction is detected. Figure 3b shows the low energy Raman shifts of pure $Eu[Ag(CN)_2]_3$ (bottom) and $Eu[Au(CN)_2]_3$ (top) with the mixed-metal complexes with decreasing silver content in between. The two bands at ∼400 $cm^{-1}$ are assigned to $\nu$(AgC) while the very weak band at ∼468 $cm^{-1}$ is assigned to $\nu$(AuC). As the Ag loading is decreased, a new band (encircled in Figure 3(b)) emerges which appears between the bands arising from $\nu$(AgC) and $\nu$(AuC) modes. We believe that the appearance of a new band is due to the influence of mixed metal interactions between Ag and Au ions to the $\nu$(AgC) mode. The $\nu$(AgC) is affected by the presence of $Au(CN)_2^-$ ions in the system and the perturbation causes broadening of the two sharp bands and then becoming a single peak. This supports that there are Ag−Au species present. In the Raman spectra (second from bottom, Figure 3b), the two bands assigned to $\nu$(AgC) are still distinct, although a peak in the middle of the two bands is shown to be emerging. The other bands in the low energy region of the Raman spectra are assigned as follows: a bending mode, $\delta$(AuCN) at ∼340 $cm^{-1}$; and at ∼285 $cm^{-1}$, $\delta$(AgCN). The change in relative intensities of the bands arising from $\delta$(AgCN) and $\delta$(AuCN) is consistent with the Ag and Au loading in the mixed metal complexes, respectively.

**2.4. Optical Studies.** The luminescence properties of europium(III) and terbium(III) ions are readily influenced by their neighbors,[39] although with the f orbitals strongly shielded from the outside ligands, the positions of the spectral lines vary only slightly with the environment. Intensities of spectral lines however are strongly dependent on the host in which the rare earth is attached.[40] The primary focus of these studies, however, is to determine if energy transfer takes place with the mixed metal $Ag/Au(CN)_2^-$ ions serving as the donor ions and the europium ion serving as the acceptor ion. The tunability of the emission energies which is due to varying the Ag/Au ratios makes this study interesting since the efficiency of energy transfer is linearly dependent on the magnitude of the spectral overlap between the donor emission and the acceptor absorption. Therefore, the shifts in maximum emission energies due to the respective Ag/Au ratios in the different $Eu^{3+}$ complexes can play an important role in energy transfer studies.

*2.4.1. Pure System Photoexcitation.* Figure 4, parts a and b, shows the excitation spectra of $Eu[Ag(CN)_2]_3$ and $Eu[Au(CN)_2]_3$ at 77 K. In Table 4, the peak assignments for the excitation bands in $Eu[Ag(CN)_2]_3$ and $Eu[Au(CN)_2]_3$ are presented. The excitation lines are classified according to literature assignments given for $Eu^{3+}$.[3,41] As can be seen, the excitation spectra present spectral lines consistent with the Eu(III) ion. When the excitation spectrum is monitored for the $Eu^{3+}$ emission line (593 nm), Figure 4a, it shows bands corresponding to f−f transitions which are observed at 376 and 398 nm. These bands arise from the $^7F_0 \rightarrow f^5L_J$ ($J = 6, 7$) transitions. Weak but sharp bands are also observed in the 400−500 nm region which corresponds to $^7F_0 \rightarrow f^5D_j$ ($j = 3, 2, 1$) transitions. The transition $^7F_0 \rightarrow f^5D_4$ is observed at 353 and 363 nm. Also, the excitation spectrum of $Eu[Ag(CN)_2]_3$ is compared with $La[Ag(CN)_2]_3$ in order to facilitate the assignment of the broad excitation band that was observed at ∼320 nm. The $La^{3+}$ complex was chosen for comparison since it does not have absorption bands and therefore would show only the bands arising from the $Ag(CN)_2^-$ ion. Comparison of the spectra shows that the 314 nm band corresponds to the $Ag(CN)_2^-$ ion. Another excitation spectrum

**TABLE 4: Assignments of Bands for the Excitation Spectrum of $Eu[Ag(CN)_2]_3$ and $Eu[Au(CN)_2]_3$ Shown in Figure 4, parts a and b**

| $Eu[Ag(CN)_2]_3$ excitation band | | | $Eu[Au(CN)_2]_3$ excitation band | |
|---|---|---|---|---|
| $\lambda$, nm | $\lambda^{-1}$, $cm^{-1}$ | assgnt | $\lambda$, nm | $\lambda^{-1}$, $cm^{-1}$ |
| 315 | 31 746 | $Ag(CN)_2^-$ | | |
| | | $Au(CN)_2^-$ | 250−450 | 40 000−22 222 |
| 353 | 28 329 | $^7F_0 \rightarrow {}^5D_4$ | 353 | 28 329 |
| 363 | 27 548 | $^7F_0 \rightarrow {}^5D_4$ | 367 | 27 247 |
| 376 | 26 595 | $^7F_0 \rightarrow {}^5L_7$ | | |
| 398 | 25 125 | $^7F_0 \rightarrow {}^5L_6$ | | |
| 406 | 24 630 | $^7F_0 \rightarrow {}^5D_3$ | 406 | 24 630 |
| 420 | 23 810 | $^7F_0 \rightarrow {}^5D_3$ | 420 | 23 810 |
| 465 | 21 505 | $^7F_0 \rightarrow {}^5D_2$ | 465 | 21 505 |
| 527 | 18 975 | $^7F_0 \rightarrow {}^5D_1$ | 527 | 18 975 |

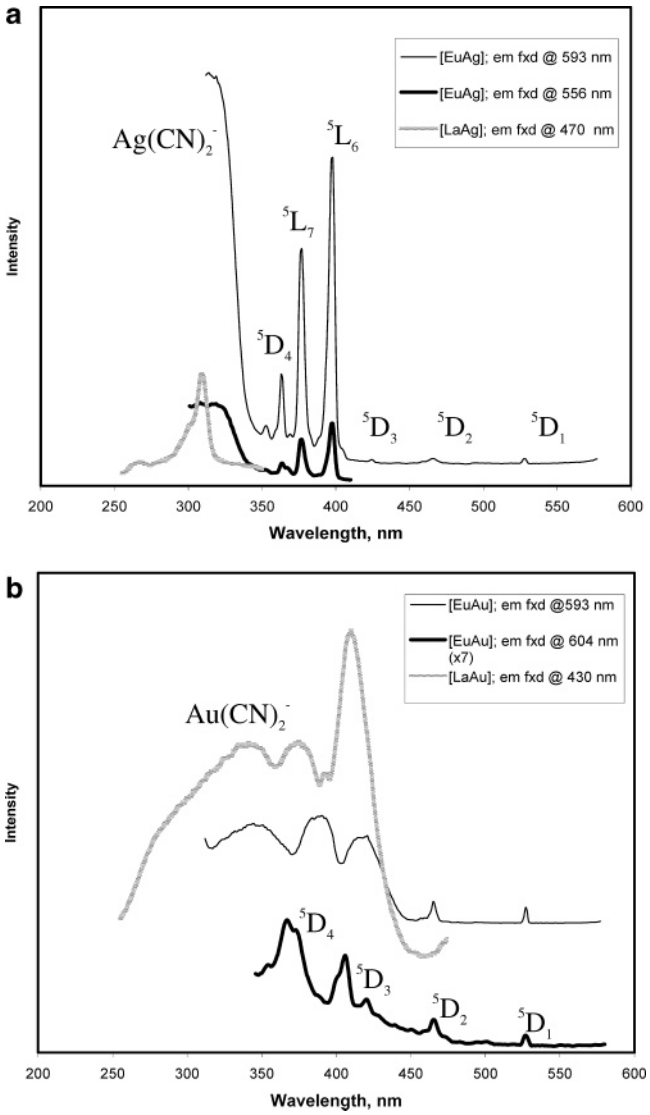


**Figure 4.** (a) Excitation spectra of $Eu[Ag(CN)_2]_3$ and $La[Ag(CN)_2]_3$ taken at 77 K. (b) Excitation spectra of $Eu[Au(CN)_2]_3$ and $La[Au(CN)_2]_3$ taken at 77 K.

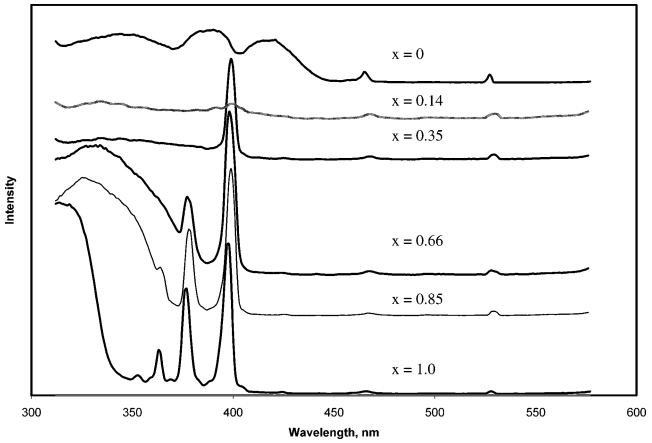


**Figure 5.** Excitation spectra of $Eu[Ag_xAu_{1-x}(CN)_2]_3$, with $x = 1.0$, 0.85, 0.66, 0.35, 0.14, and 0 with $\lambda_{em} = 594$ nm, $T = 77$ K.

($\lambda_{em} = 556$ nm, another $Eu^{3+}$ emission line) is presented to show clearly the presence of the $Ag(CN)_2^-$ band in the same region with that in the $La[Ag(CN)_2]_3$ spectra. The excitation spectrum of $Eu[Au(CN)_2]_3$, Figure 4b, shows broad excitation bands in the region where bands arising from the $^7F_0 \rightarrow f^5L_J$ transitions are expected. The excitation bands have their peak maxima at 345, 389, and 418 nm, respectively. These bands have been assigned to $Au(CN)_2^-$ ions upon comparison to the excitation spectra for $La[Au(CN)_2]_3$. Peaks due to the $^7F_0 \rightarrow f^5D_J$ ($J = 4, 3, 2, 1$) transitions are observed in the 350−600 nm region. These peaks are observed when the fixed emission wavelength is set to 430 nm. However, the intensities of the bands are weak hence the spectra is magnified 7× and is shown below the two main spectra. The peak due to the $^7F_0 \rightarrow f^5D_3$ as well as $^7F_0 \rightarrow f^5D_4$ transition is enveloped by the peaks arising from the $Au(CN)_2^-$ ions.

*2.4.2. Mixed Metal System Photoexcitation.* Figure 5 shows the excitation of the mixed metal Eu complexes along with the pure Ag and Au systems, at 77 K. It was observed that there is a correlation between the excitation bands present in the excitation spectra to the Ag and Au loading in the Eu mixed metal complex. In fact, just by looking at the spectral features, it is recognizable which metal (Ag or Au) loading is higher in the sample. The samples with more of the Ag or Au loading have the excitation spectra resembling that of the $Eu[Ag(CN)_2]_3$ spectra or $Eu[Au(CN)_2]_3$ spectra as the case may be. As the Au loading increases, the band arising from the $Ag(CN)_2^-$ transition (315 nm) broadens and red shifts occur resembling the excitation band due to the $Au(CN)_2^-$ transition. As a result, a noticeable trend occurs which is the "disappearance" of the excitation bands that are due to the $^7F_0 \rightarrow f^5L_J$ as well as the $^7F_0 \rightarrow f^5D_3$ transitions. These states are particularly significant for a later section on energy transfer studies since these are the primary acceptor states in the $Eu^{3+}$ ion.

*2.4.3. Pure System Photoluminescence.* Illumination of $Eu[Ag(CN)_2]_3$ vs $Eu[Au(CN)_2]_3$ at 4, 77, or 298 K produces red emission featuring sharp peaks typical of $Eu^{3+}$ ($^5D_0$) → $Eu^{3+}$ ($^7F_J$: 0−4).

It is interesting to note that the $[Au(CN)_2]^-$ emission in pure $Eu[Au(CN)_2]_3$ has been observed at 4 K. Two peaks have been observed at 405 and 452 nm. These peaks have not been observed in previous experiments[20b] although Yersin[3] has reported from his calculations that the peak areas would be located at 23 600 ± 300 $cm^{-1}$ (~424 nm) and pressure application resulted in the observance of the peak. Emission bands due to $[Ag(CN)_2]^-$ have been observed at 283 nm along with a broad band with a peak maximum at 349 nm. The pure

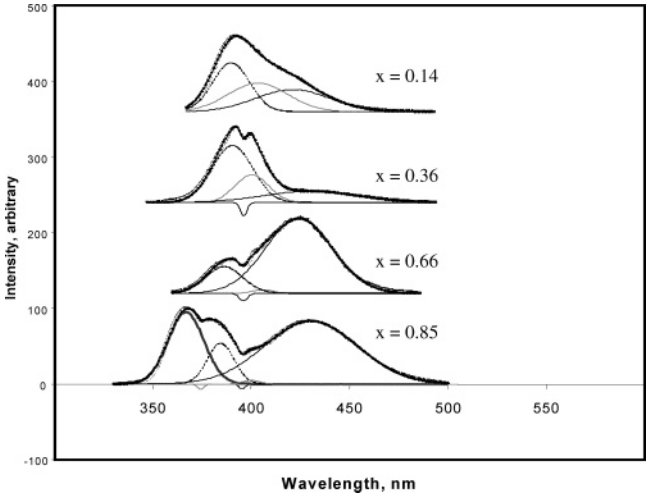


**Figure 6.** Emission spectra of $Eu[Ag_xAu_{1-x}(CN)_2]_3$, with $x = 0.85$, 0.66, 0.35, and 0.14 with $\lambda_{exc} = 290$ nm, $T = 77$ K. Presented along with the raw data (wide pale line) for each complex is the fit and the Gaussian functions comprising the fit. The spectra show the Ag(I), Au(I), and Ag(I)−Au(I) mixed metal emission region.

**TABLE 5: Assignments of Bands for the Emission Spectrum of the Mixed Metal Complexes Shown in Figure 6**

| complex\λ$_{nm}$ (max) | $*[Ag(CN)_2]_n^-$ | $*[Ag_xAu_{1-x}(CN)_2]_n^-$ | $*[Au(CN)_2]_n^-$ |
|---|---|---|---|
| $Eu[Ag_{0.85}Au_{0.15}(CN)_2]_3$ | 367, 430 | 384 | 400 |
| $Eu[Ag_{0.66}Au_{0.34}(CN)_2]_3$ | 424 | 386 | 406 |
| $Eu[Ag_{0.35}Au_{0.65}(CN)_2]_3$ | 430 | 390 | 400 |
| $Eu[Ag_{0.14}Au_{0.86}(CN)_2]_3$ | 421 | 390 | 403 |

silver and gold Eu(III) complex emission intensities were weak and the presence of the emission bands were only observed at 4 K.

*2.4.4. Mixed Metal System Photoluminescence.* It is interesting to note that the emission bands for the different mixed metal ratios, shown in Figure 6, although exhibiting slight red shifts in the peak maxima, have emission energies similar to each other. The bandwidth is where there is a disparity from one mixed metal complex to the next. Eu(III) mixed metal complexes exhibit two visible major broad emission bands. This is in sharp contrast to the mixed metal peaks observed in the La complex which shows only one major peak.[6] Additionally, in the case of La mixed metal system that was studied primarily to characterize the interaction between the gold and silver ions, it was reported that there is a distinct peak shift to either the Ag or the Au side depending on which metal is contained more in the complex. This suggests that there is a better mixed metal interaction of Au−Ag in the La complexes as compared to the Eu complexes.

The emission spectra were analyzed to determine how many Gaussian functions fit the raw data. For all of the samples' steady-state luminescence data, fits of the spectra were made to three or more Gaussian functions. Presented in Table 5 are the assignments corresponding to the emission bands for the Gaussian functions that comprise the fit of the raw data. Figure 6 shows the emission spectra of the mixed metal complexes along with the Gaussian function fit for each complex. The emission peaks at ~367 and ~430 nm arises due to $*[Ag(CN)_2]_n^-$. It should be noted that the presence of the peak at ~367 nm is only distinctly observable with the Eu mixed metal complex containing high amounts of the $Ag(CN)_2^-$ ions, i.e., $Eu[Ag_{0.85}Au_{0.15}(CN)_2]_3$. This is similar with the La complexes where only the $La[Ag_{0.79}Au_{0.21}(CN)_2]_3$ shows the higher energy peak. The peak at ~400 nm is due to $*[Au(CN)_2]_n^-$. The emission peak at ~380 nm is assigned to the Ag−Au mixed

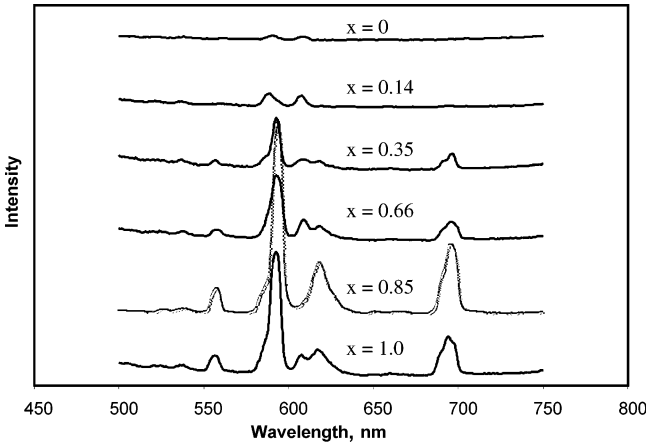


**Figure 7.** Emission spectra of $Eu[Ag_xAu_{1-x}(CN)_2]_3$, with $x = 1.0$, 0.85, 0.66, 0.35, 0.14, and 0 with $\lambda_{ex} = 400$ nm, $T = 298$ K. The spectra show the Eu(III) emission region.

metal complex. This is a significant peak since it has been observed to influence the efficiency of energy transfer and this is discussed in a later section. With a decrease in temperature (4 K), the peak positions have a slight red shift with the spectral features more defined. Additionally, the appearance of broad band at a higher wavelength has been observed, although it has very weak intensity.

Figure 7 shows the emission bands due to $Eu^{3+}$ ($^5D_0$) → $Eu^{3+}$-($^7F_J$: 0−4) transitions of the Eu(III) mixed metal systems along with the pure Eu(III) systems. These measurements were carried out at room temperature with a fixed excitation wavelength of 400 nm. The figure shows that at room temperature, $Eu[Au(CN)_2]_3$ does not have a strong emission intensity, with only the appearance of emission bands arising from $Eu^{3+}$ ($^5D_0$) → $Eu^{3+}$($^7F_J$: 1,2) transitions. On the other hand, the emission intensity for $Eu[Ag(CN)_2]_3$ was strong with the presence of different emission peaks from the different Eu(III) transitions.

*2.4.5. Energy Transfer.* In energy transfer studies, an important factor in considering donor and acceptor systems has been the degree of spectral overlap between the acceptor's absorption states and the donor's emission states. Mathematically, the energy transfer rate, $P_{D-A}$, can be expressed in terms of the spectral overlap integral between the emission (*e*) of the donor (D) and the absorption (*a*) of the acceptor (A) as shown in the equation below:[3,42]

$$P_{D-A} = F(R) \int f^e_D(\bar{v}) f^a_A(\bar{v})\, d\bar{v} \qquad (1)$$

The integral is the important spectral overlap integral of the donor emission $f^e_D(\bar{v})$ with the acceptor absorption profile $f^a_A(\bar{v})$. Both functions are normalized according to $\int f^e_D(\bar{v})\, d\bar{v} = \int f^a_A(\bar{v})\, d\bar{v} = 1$. The factor $F(R)$ contains information about the mechanism of energy transfer, as well as the distance between the donor and acceptor. In dicyanoargentate(I) and dicyanoaurate(I) systems, it has been established[2b,3] that, due to the short donor−acceptor distance and the character of the luminescence decay of the donor, the dominant mechanism of energy transfer is the Dexter exchange mechanism.

Figure 8 shows the large spectral overlap between the [Ag/$Au(CN)_2^-$] donor emission respectively and the Eu(III) acceptor absorption at 77 K. This spectral overlap occurs over a rather broad spectral range due to the several emission centers of the $[Ag_x/Au_{1-x}(CN)_2]^-$ donor ions that coincide with the absorption bands of the acceptor. These emission centers are attributed to different excited-state oligomers (exciplexes) of *[$Ag(CN)_2^-$]

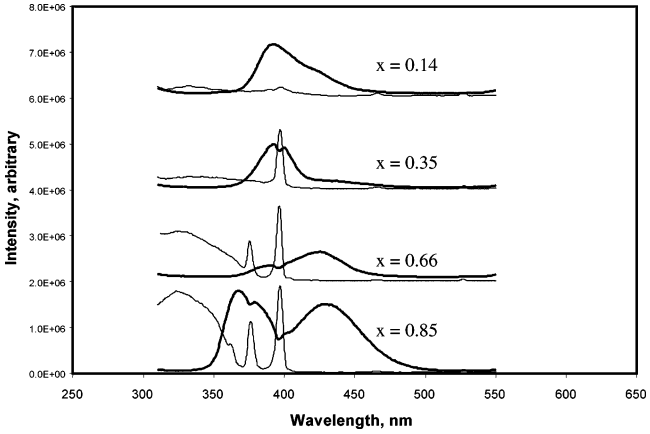


**Figure 8.** Spectral overlap between the [Ag/$Au(CN)_2^-$] donor emission (bold) and the Eu(III) excitation at 77 K.

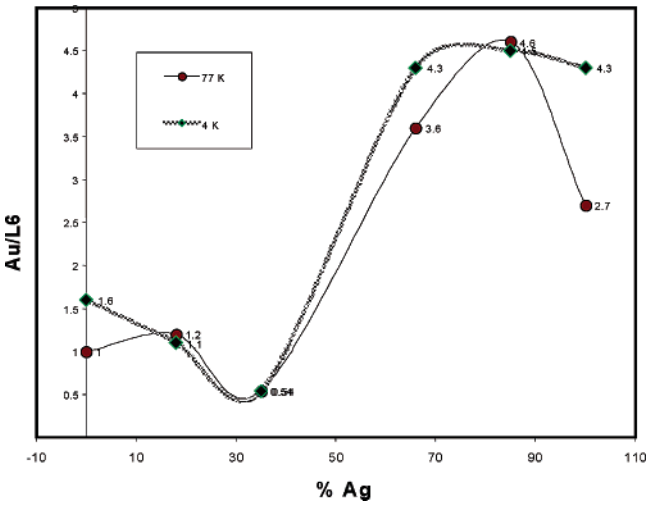


**Figure 9.** Eu(III) emission peak area (594 nm) ratios upon excitation at the $d^{10}$ Au/Ag absorption energy vs $^5L_6$ Eu(III) state.

and *[$Au(CN)_2^-$] species.[4a,43] Eu(III) mixed metal samples with higher Ag loading ($Eu[Ag_{0.85}Au_{0.15}(CN)_2]_3$ and $Eu[Ag_{0.66}Au_{0.34}(CN)_2]_3$) as expected has spectral features showing the Ag character. In Figure 9, it shows that $Eu[Ag_{0.85}Au_{0.15}(CN)_2]_3$ has the largest area of overlap between the donor emission and the acceptor absorption. This is due to the high silver ion content which allows emission energies to be observed at higher energies. The large overlap includes all of the $^5L_6$, $^5L_7$, and $^5D_J$ ($J = 3$, 2) states. The Eu(III) mixed metal samples with more Au loading ($Eu[Ag_{0.35}Au_{0.65}(CN)_2]_3$ and $Eu[Ag_{0.14}Au_{0.86}(CN)_2]_3$) have a small overlap. This is due in part to the merging of the peaks that have been distinctly separate in the mixed metal complexes with high Ag loading.

In Table 6, the values from calculations of the energy transfer rates using eq 1 are given. The calculations did not include the $F(R)$ quantity with the assumption that all of the samples have the same energy transfer mechanism since they are similar complexes. Data from the photoexcitation studies were used instead of the acceptor absorption integral for the acceptor ions. The transfer rate was calculated for each peak comprising the fit for the donor emission (see Figure 6, Table 5) to identify which emissive cluster has a high efficiency for energy transfer. For comparison purposes, the data presented in Table 6 are scaled so that the sum of the energy transfer rates will equal one. Data comparison is only within each sample. The results of calculations show that they are in agreement with the above

**TABLE 6: Energy Transfer Rates for Emission Peaks in the Mixed Metal Complexes**

| complex\donor peak | $*[Ag(CN)_2]_n^-$ $\lambda_{max} = \sim 367$ nm | $*[Ag_xAu_{1-x}(CN)_2]_n^-$ $\lambda_{max} = \sim 380$ nm | $*[Au(CN)_2]_n^-$ $\lambda_{max} = \sim 400$ nm | $*[Ag(CN)_2]_n^-$ $\lambda_{max} = \sim 420$ nm |
|---|---|---|---|---|
| $Eu[Ag_{0.85}Au_{0.15}(CN)_2]_3$ | 0.44 | 0.23 | 0.03 | 0.30 |
| $Eu[Ag_{0.66}Au_{0.34}(CN)_2]_3$ | | 0.51 | 0.02 | 0.47 |
| $Eu[Ag_{0.35}Au_{065}(CN)_2]_3$ | | 0.60 | 0.34 | 0.06 |
| $Eu[Ag_{0.14}Au_{0.86}(CN)_2]_3$ | | | | |

**TABLE 7: Eu(III) Emission Peak Area (594 nm) Ratios upon Excitation at the $d^{10}$ Au/Ag Absorption Energy vs $^5L_6$ Eu(III) State**

| | $Eu[Ag(CN)_2]_3$ | $Eu[Ag_{0.85}Au_{0.15}(CN)_2]_3$ | $Eu[Ag_{0.66}Au_{0.34}(CN)_2]_3$ | $Eu[Ag_{0.35}Au_{0.65}(CN)_2]_3$ | $Eu[Ag_{0.14}Au_{0.86}(CN)_2]_3$ | $Eu[Au(CN)_2]_3$ |
|---|---|---|---|---|---|---|
| 77 K | 2.7 | 4.6 | 3.6 | 0.54 | 1.2 | 1.0 |
| 4 K | 4.3 | 4.5 | 4.3 | 0.54 | 1.1 | 1.6 |

discussion. The samples that contain $*[Ag(CN)_2^-]_n$ have the greatest energy transfer rates.

The presence of the donor excitation profile along with the acceptor lines in the excitation spectra is indicative of energy transfer. This method has been used to confirm the presence of energy transfer in many biochemical[44−49] and inorganic systems.[2b,20a,50−52] To determine whether the presence of the donor ions had an effect on the emission intensity of the Eu(III) emission through energy transfer, luminescence experiments were carried out where excitation at the donor maximum excitation peak was compared with excitation at the Eu(III) excitation wavelength. The data presented in Table 7 results from the following equation:

$$\text{ratio of Eu(III) peak area (594 nm)} = \frac{\text{peak area exc fixed } d^{10} \text{ wavelength}}{\text{peak area exc fixed } {}^5L_6 \text{ wavelength}} \quad (2)$$

Figure 9 shows the graphical representation of Table 7. The numbers presented in the table are the ratio of the Eu emission peak area when it was excited at the $d^{10}$ absorption over the emission area when it was excited at the donor excitation wavelength. The data indicates that samples with the higher silver loading have a more efficient energy transfer since Eu emission is more intense when excited at the donor excitation wavelength which suggests that there is significant interaction between the donor and acceptor ions. $Eu[Ag_{0.35}Au_{0.65}(CN)_2]_3$ has numbers less than one which tells that the presence of the donor ions have an insignificant effect on the emission intensity of the Eu(III) peaks. This suggests that energy transfer is not efficient in this particular sample. This may be due to the fact that since there is a high interaction between the Ag(I) and Au(I) ions, as observed from the strong intensity of the Gaussian function assigned to the Ag−Au emission peak (Figure 6), the mixed metal interaction competes with the $Au(CN)_2^- \rightarrow$ Eu(III) or $Ag(CN)_2^- \rightarrow$ Eu(III) energy transfer processes. Another possibility is that another energy transfer process occurs from the $Ag(CN)_2^-$ with the $Ag_xAu_{1-x}(CN)_2^-$ entity as the acceptor component.

This analysis has also been used to identify which is the primary acceptor state, whether it is the $^5L_J$ or the $^5D_J$ ($J = 3$, 2, 1, 0) states. Results reveal that $^5L_J$ is the primary acceptor state. A possibility exists that, after UV excitation, the $^5D_J$ states are not effectively occupied and only after relaxation does it populate the $^5D_J$ states. Studies wherein these effects have been investigated have been carried out with Pt(II) and Ru(II) complexes.[53] Notice too that pure silver and mixed metal complexes with a higher silver loading have better energy transfer efficiency than the pure gold complex. One of the reasons is that there are more acceptor states involved with the silver complexes. In the gold sample, this is due to the fact that the gold absorption and the $^5L_6$ states have similar energies. To have higher energy transfer efficiency, the lowest triplet energy state of the donor should be higher in energy than the luminescent state of the acceptor lanthanide ion, both to fulfill the energetic requirements and to ensure a fast and irreversible energy transfer.[54]

## 3. Conclusions

Studies have been reported for the first time on the novel layered heterobimetallic system, $Eu[Ag_xAu_{1-x}(CN)_2]_3$ ($x = 0.90$, 0.75, 0.50, and 0.25). Energy transfer occurs from the tunable $[Ag_xAu(CN)_2]^-$ donor ions to the luminescent $Eu^{3+}$ acceptor ions with the energy tunability of the donor ions dependent on the Ag/Au stoichiometric ratio. Metallophilic interactions have been probed with crystallographic and Raman studies.

The results of studies of the mixed metal complexes have been compared with those on pure crystals of Eu(III) dicyanoaurate(I) and dicyanoargentate(I). Mixed metal complexes with more silver loading than gold have excitation spectral features such as the pure silver complex and the complexes with more gold loading have the pure gold characteristics. Emission bands assigned to mixed metal clusters of $Au(CN)_2^-$ and $Ag(CN)_2^-$ have been observed. The mixed metal systems with the higher loading of silver, $Eu[Ag_{0.85}Au_{0.15}(CN)_2]_3$ and $Eu[Ag_{0.66}Au_{0.34}(CN)_2]_3$, have better energy transfer than the mixed metal systems with less silver, $Eu[Ag_{0.35}Au_{0.65}(CN)_2]_3$ and $Eu[Ag_{0.14}Au_{0.86}(CN)_2]_3$. This is due to the greater extent of overlap between the donor emission and the acceptor absorption in the complexes with the higher silver loading. With the better overlap, it results in having more acceptor states available for the $Eu^{3+}$ ion involved in the energy transfer processes.

X-ray diffraction studies provide support that energy transfer can occur in the Eu(III) mixed metal complexes because of the short bond distances between the pertinent atoms, comparable to the bond distances of the atoms found in the pure silver Eu(III) complex wherein energy transfer processes have been established to occur. The Raman studies provide further evidence to support the results from luminescence measurements that there are Ag−Au interactions in the mixed metal Eu(III) complexes. The presence of the mixed metal interactions are significant because of competition with the energy transfer processes occurring between Ag(I) donor ions and the Eu(III) acceptor ions as well as between Au(I) donor ions and the Eu(III) acceptor ions.

Energy transfer processes have again been observed to occur in the pure silver and gold Eu(III) complexes, in agreement with

previous studies.[3,20a] In comparing the pure systems, it has been observed that the pure silver complex has a higher energy transfer efficiency than the gold case. Although both pure systems have good overlap between their respective emission bands and the Eu(III) acceptor states, in the case of the pure gold complex, the possibility of back transfer offsets the efficiency of energy transfer since the absorption energies of the $Au(CN)_2^-$ ions lies at the same energies as the $^5L_6$ absorption state of the $Eu^{3+}$ ions. Results reveal that the $^5L_6$ state is the primary acceptor state.

**Acknowledgment.** This work was supported by the American Chemical Society, Petroleum Research Fund.

## References and Notes

(1) (a) Rawashdeh-Omary, M. A.; Omary, M. A.; Patterson, H. H.; Fackler, J. P., Jr. *J. Am. Chem. Soc.* **2001**, *123*, 11237. (b) Rawashdeh-Omary, M. A.; Omary, M. A.; Patterson, H. H. *J. Am. Chem. Soc.* **2000**, *122*, 10371.

(2) (a) Rawashdeh-Omary, M. A.; Omary, M. A.; Shankle, G. E.; Patterson, H. H. *J. Phys. Chem. B* **2000** *104*, 6143. (b) Rawashdeh-Omary, M. A.; Larochelle, C. L.; Patterson, H. H. *Inorg. Chem.* **2000**, *39*, 4527.

(3) Yersin, H.; Trümbach, D.; Strasser, J.; Patterson, H. H.; Assefa, Z. *Inorg. Chem.* **1998**, *37*, 3209.

(4) (a) Omary, M. A.; Patterson, H. H. *J. Am. Chem. Soc*. **1998**, *120*, 7696. (b) Patterson, H. H.; Kanan, S. M.; Omary, M. A. *Coord. Chem. Rev.* **2000**, *208*, 227.

(5) Omary, M. A.; Hall, D. R.; Shankle, G. E.; Siemiarczuk, A.; Patterson, H. H. *J. Phys. Chem. B* **1999**, *103*, 3845.

(6) Colis, J. C. F.; Larochelle, C. L.; Fernández, E. J.; López-de-Luzuriaga, J. M.; Monge, M.; Laguna, A.; Tripp, C.; Patterson, H. H. *J. Phys. Chem. B* **2004**, *submitted*.

(7) Yersin, H.; Gliemann, G. *Ann. N.Y. Acad. Sci.* **1978**, *313*, 539.

(8) Gliemann, G.; Yersin, H. *Struct. Bond*. **1985**, *62*, 87.

(9) Cummings, S. D.; Eisenberg, R. *J. Am. Chem. Soc*. **1996**, *118*, 1949.

(10) Mayer, A.; Neuenhofer, S. *Angew. Chem., Int. Ed. Engl.* **1994**, *33*, 1044.

(11) (a) Hehlen, M. P.; Krämer, K.; Güdel, H. U.; McFarlane, R. M.; Schwartz, R. N. *Phys. Rev. B* **1994**, *49*, 12475. (b) Riedener, T.; Krämer, K.; Güdel, H. U. *Inorg. Chem.* **1995**, *34*, 2745.

(12) Maas, H.; Currao, A.; Calzaferri, G. *Angew. Chem., Int. Ed. Engl.* **2002**, *41*, 2495.

(13) (a) Van der Tol, E. B.; van Ramesdonk, H. J.; Verhoeven, J. W.; Steemers, F. J.; Kerver, E. G.; Verboom, W.; Reinhoudt, D. N. *Chem. Eur. J.* **1998**, *4*, 2315. (b) Klink, S. I.; Keizer, H.; van Veggel, F. C. J. M. *Angew. Chem., Int. Ed. Engl.* **2000**, *39*, 4319.

(14) (a) Li, Q.; Li, T.; Wu, J. *J. Phys. Chem. B.* **2001**, *105*, 12293. (b) Gonçalves e Silva, F. R.; Malta, O. L.; Reinhard, C.; Güdel, H.-U.; Piguet, C.; Moser, J. E.; Bünzli, J.-C. G. *J. Phys. Chem. A.* **2002**, *106*, 1670. (c) Song, H.; Lu, S.; Renxi Gao, S. E.; Zhang, J. H.; Chen, B. *J. Appl. Phys.* **2002**, *91*, 2959. (d) Moadhen, A.; Elhouichet, H.; Oueslati, M.; Férid, M. *J. Lumin.* **2002**, *99*, 13.

(15) (a) Frindell, K. L.; Bartl, M. H.; Popitsch, A.; Stucky, G. D. *Angew. Chem., Int. Ed. Engl.* **2002**, *41*, 960. (b) Pagnot, T.; Barchiesi, D.; Tribillon, G. *Appl. Phys. Lett.* **1999**, *75*, 4207. (c) Sun, P.-P.; Duan, J.-P.; Shih, H.-T.; Cheng, C.-H. *Appl. Phys. Lett.* **2002**, *81*, 792.

(16) Okamoto, S.; Kobayashi, M.; Kanemitsu, Y.; Kushida, T. *Phys. Stat. Sol. B.* **2002**, *1*, 481.

(17) (a) Diaz-Garcia, M. A.; Fernandez De Avila, S.; Kuzyk, M. G. *Appl. Phys. Lett.* **2002**, *81*, 3924. (b) Sokolnocki, J.; Legendziewicz, J.; Riehl, J. P. *J. Phys. Chem. B* **2002**, *106*, 1508.

(18) Tallant, D. R.; Seager, C. H.; Simpson, R. L. *J. Appl. Phys.* **2002**, *91*, 4053.

(19) Thompson, M. K.; Vuchkov, M.; Kahwa, I. A. *Inorg. Chem.* **2001**, *40*, 4332.

(20) (a) Assefa, Z.; Shankle, G.; Patterson, H. H.; Reynolds, R. *Inorg. Chem.* **1994**, *33*, 2187 (b) Assefa, Z.; Patterson, H. H. *Inorg. Chem.* **1994**, *33*, 3, 6194.

(21) Patterson, H. H.; Roper, G.; Biscoe, J.; Ludi, A.; Blom N. *J. Lumin.* **1984**, *31/32*, 555.

(22) Markert, J. T.; Blom, N.; Roper, G.; Perregaux, A. D.; Nagasundaram, N.; Corson, M. R.; Ludi, A.; Nagle, J. K.; Patterson, H. H. *Chem. Phys. Lett.* **1985**, *118*, 258.

(23) Nagle, J. K.; LaCasce, J. H., Jr.; Dolan, P. J., Jr.; Corson, M. R.; Assefa, Z.; Patterson, H. H. *Mol. Cryst. Liq. Cryst.* **1990**, *181*, 359.

(24) Assefa, Z.; DeStefano, F.; Garepapaghi, M. A.; LaCasce, J. H., Jr.; Ouellette, S.; Corson, M. R.; Nagle, J. K.; Patterson, H. H. *Inorg. Chem.* **1991**, *30*, 2868.

(25) Fischer, P.; Ludi, A.; Patterson, H. H.; Hewat, A. W. *Inorg. Chem.* **1994**, *33*, 62.

(26) Fischer, P.; Mesot, J.; Lucas, B.; Ludi, A.; Patterson, H. H.; Hewat, A. *Inorg. Chem.* **1997**, *36*, 2791.

(27) LaCasce, J. H., Jr.; Turner, W. A.; Corson, M. R.; Dolan, P. J., Jr.; Nagle, J. K. *Chem. Phys.* **1987**, *118*, 289.

(28) Patterson, H. H. Electronic and Vibronic Spectra of Transition Metal Complexes. II; Yersin, H., Ed., In *Topics in Current Chemistry*; Springer-Verlag: Berlin, 1997; Vol. 191.

(29) (a) Yersin, H.; Riedl, U. *Inorg. Chem.* **1995**, *34*, 1642. (b) Rosenzweig, A.; Cramer, D. T. *Acta Crystallogr.* **1959**, *12*, 709.

(30) Rosenzweig, A.; Cramer, D. T. *Acta Crystallogr.* **1959**, *12*, 709.

(31) Blom, N.; Ludi, A.; Bürgi, H.-B.; Tichy, K. *Acta Crystallogr.* **1984**, *C40*, 1767.

(32) Blom, N.; Ludi, A.; Bürgi, H.-B. *Acta Crystallogr.* **1984**, *C40*, 1770.

(33) Assefa, Z.; Staples, R.; Fackler, Jr., J. P.; Patterson, H. H.; Shankle, G.; *Acta Crystallogr.* **1995**, *C51*, 2527.

(34) Nyquint, R. A.; Putzig, M. A.; Leugers, M. A. In *The Handbook of Infrared and Raman Spectra of Inorganic Compounds and Organic Salts*; Academic Press: San Diego, 1997; Vol. 2.

(35) Bottger, G. L. *Spectrochim. Acta* **1968**, *24A*, 1821.

(36) Jones, L. H. *Spectrochim. Acta* **1963**, *19*, 1675.

(37) Adams, D. M.; Fletcher, P. A. *Spectrochim. Acta* **1988**, *44A*, 437.

(38) Stammreich, H.; Chadwick, B. M.; Frankiss, S. G. *J. Mol. Struct.* **1967**, *1*, 191.

(39) (a) Kahwa, I. A.; Parkes, C. C.; McPherson, G. L. *Phys. Rev.* **1995**, B52, 1177. (b) Richardson, F. S. *Chem. Rev.* **1982**, *82*, 541. (c) Horrocks, W. deW., Jr.; Sudnick. D. R. *Acc. Chem. Res.* **1981**, *14*, 384. (d) Piguet, C.; Bünzli, J.-C. G.; Bernardinelli, G.; Hopfgartner, G. Petoud, S.; Shaad, O. *J. Am. Chem. Soc*. **1996**, *118*, 6681. (e) Gunnlaugsson, T.; MacDo'nail, D. A.; Parker, D. *Chem. Commun.* **2000**, 93.

(40) (a) Reisfeld, R.; Saraidarov, T.; Ziganski, E.; Gaft, M.; Lis, S.; Pietraszkiewicz, M. *J. Lumin.* **2003**, *102*−*103*, 243.

(41) Kodaira, C. A.; Britoa, H. F.; Malta, O. L.; Serra, O. A. *J. Lumin.* **2003**, *101*, 11.

(42) Dexter, D. L. *J. Chem. Phys.* **1953**, *21*, 836.

(43) Hettiarachchi, S. R.; Rawashdeh-Omary, M. A.; Kanan, S. M.; Omary, M. A.; Patterson, H. H.; Tripp, C. P. *J. Phys. Chem. B* **2002**, *106*, 10058.

(44) Monasterio, O.; Acoria, M.; Díaz, M. A.; Lagos, R. *Arch. Biochem. Biophys.* **1993**, *300*, 582.

(45) Sherry, A. D.; Au−Young, S.; Cottam, G. L. *Arch. Biochem. Biophys.* **1978**, *189*, 277.

(46) Rübsamen, H.; Hess, G. P.; Eldefrawi, A. T.; Eldefrawi, M. E. *Biochem. Biophys. Res. Commun.* **1976**, *68*, 56.

(47) Luk, C. K. *Biochemistry* **1971**, *10*, 2838.

(48) Richardson, C. E.; Behnke, W. D. *Biochim. Biophys. Acta* **1978**, *534*, 267.

(49) Ringer, D. P.; Etheredge, J. L.; Dalrymple, B. L.; Niedbalski, J. S. *Biochem. Biophys. Res. Commun.* **1990**, *168*, 267.

(50) Blasse, G.; Bokkers, G.; Dirksen, G.; Brixner, L. *J. Solid State Chem.* **1983**, *60*, 803.

(51) Chang, N. C. *J. Appl. Phys.* **1963**, *34*, 3500.

(52) de Hair, J. T. W. *J. Lumin.* **1979**, *18/19*, 797.

(53) Schmidt, J.; Strasser, J.; Yersin, H. *Inorg. Chem.* **1997**, *36*, 3957.

(54) Bünzli, J.-C. G. Luminescent Probes; Bünzli, J.-C. G., Choppin, G. R., Ed.; In *Lanthanide Probes in Life, Chemical and Earth Sciences*; Elsevier: Amsterdam, 1989; p 219.